



RESEARCH PAPER

OPEN ACCESS

Anticarcinogenic and antimicrobial assessment of copper oxide nanoparticles derived from the leaf extract of *Catharanthus roseus*

Selvanayakam Sumitha, Esakiappan Subramanian, Kalaiyar Swarnalatha*

*Photochemistry Research Laboratory, Department of Chemistry,
Manonmaniam Sundaranar University, Abishekapatti, Tirunelveli, Tamil Nadu, India*

Article published on February 18, 2024

Key words: Copper oxide nanopartiles, Leaf extract, Antibacterial, Antifungal, Antioxidant, Anticancer activity

Abstract

This study focuses on the biological examination of copper oxide nanoparticles (CuO NPs) synthesized using *Catharanthus roseus* leaf extract, which served both as reducing and stabilizing agents. The formation of these biogenic CuO NPs was analyzed through UV-visible, Fourier transform infrared spectroscopy (FTIR), X-ray diffraction (XRD), and scanning electron microscopy (SEM). The UV-visible spectral analysis revealed a peak at 273 nm, while FTIR provided insight into the functional groups associated with the NPs. Antibacterial testing showed inhibition zones (ZOI) and Minimum Inhibitory Concentration (MIC) against eight pathogenic bacterial strains, both positive and negative. Antifungal testing exhibited ZOI against four pathogenic fungal organisms. Furthermore, the nanoparticles displayed antioxidant potential, with an IC₅₀ value of 58.55 µg/ml, indicating the scavenging ability. The in-vitro assessment of anticancer activity was carried out against the HT29 cell line, revealing an IC₅₀ value of 37.99 µg/ml.

*Corresponding Author: Kalaiyar Swarnalatha ✉ swarnalatha@msuniv.ac.in

Introduction

Nanoparticles have indeed revolutionized various fields due to their unique properties and applications. In pharmaceuticals, NPs are used to enhance drug delivery by improving solubility, bioavailability, and targeting specific areas in the body (Bajwa *et al.*, 2023). Nanoparticles come in various forms metallic (like gold, silver, iron) and non-metallic (like carbon-based or polymer-based). Their size and properties can be finely tuned for specific applications, making them versatile tool across scientific disciplines (Sajid and Plotka-Wasyłka, 2020; Jabarkhil *et al.*, 2023; Saleh and Hassan, 2023). For the past two decades, numerous researchers have explored the synthesis of metallic nanoparticles utilizing various metals such as iron, silver, gold, manganese, copper, zinc and more (Gahlawat and Choudhury, 2019; Darroudi *et al.*, 2011). Similarly, Sardar *et al.* and Thambidurai *et al.* reported the biological and physicochemical properties of green metal and metal oxide nanoparticles using conventional methods (Sardar *et al.*, 2022; Thambidurai *et al.*, 2020). Among these, copper oxide nanoparticles (CuO NPs) have piqued researchers' interest due to their potential applications in cellular targeting and drug delivery, due to their excellent magnetic properties (Rajagopal *et al.*, 2021).

In recent times, copper oxide nanoparticles (CuO NPs) have been widespread utilization across a spectrum of items, including personal care products, food storage containers, household appliances, paints, textiles, batteries, catalysis, gas sensors, and tools for electrical, optical and solar energy applications (Siddiquee *et al.*, 2021). The creation of nanoparticles through chemical means is expensive, showcasing only moderate anti-cancer capabilities while potentially affecting healthy cells. In contrast, using biosynthesized nanomaterials for cancer treatment has resulted in minimal side effects and toxicity, leading to enhanced targeted cell therapy. Metal and metal oxide nanoparticles have emerged as promising agents for combating various types of cancer cells effectively (Manimaran *et al.*,

2023). Many researchers covered various aspects of CuO nanoparticles, including synthetic methods, characterization, applications in different fields, and their effects in areas like antibacterial activity and water treatment (Jadhav *et al.*, 2011; Chakraborty *et al.*, 2022; Bhavyasree and Xavier, 2022; Alahdal *et al.*, 2023).

The current research aimed to evaluate the antimicrobial, antioxidant, and anticancer potential of CuO NPs synthesized through green methods using *Catharanthus roseus* leaf extract. These nanoparticles were tested against pathogenic bacteria and human colon cancer cells in laboratory conditions.

Materials and methods

Materials required

Catharanthus roseus leaves were collected from our University campus, Tirunelveli. Cupric chloride (99%) procured from Merck, Mumbai. All solutions were prepared by using distilled water. *Bacillus cereus*, *Streptococcus pyogenes*, *Pseudomonas aeruginosa*, *Staphylococcus aureus*, *Propionibacterium acnes*, *Actinomyces israelii*, *Streptococcus faecalis*, *Enterococcus faecalis* were purchased from MTCC, Chandigarh, India. Nutrient broth, Gentamicin antibiotic solution, Potato dextrose agar medium, Amphotericin B antimycotic solution, 1X PBS were purchased from Himedia, India. DMEM medium, Fetal Bovine Serum (FBS) and antibiotic solution were from Gibco (USA), DMSO (Dimethyl sulfoxide) and MTT (3,4,5 dimethylthiazol-2-yl-2,5-diphenyl tetrazolium bromide) were procured from Sigma, USA. HT-29 (human colon cancer cell line) were purchased from NCCS, Pune. Microplate reader was purchased from Thermo Fisher Scientific, USA and all solutions were prepared by using distilled water.

Preparation of leaf extract

The fresh leaves (50-100 no's) of *Catharanthus roseus* were washed with distilled water. The washed leaves were heated to boil and the leaf extract was obtained as yellowish green colour. The extract was collected in a 100 mL beaker for further use.

Synthesis of CuO NPs

About 0.17 gm of $\text{CuCl}_2 \cdot 2\text{H}_2\text{O}$ precursor was added with the 25 mL of leaf extract in a 250 mL Erlenmeyer flask. It is heated to about 60°C - 80°C and continuous stirring for 30 mins. The colour of the solution changes to pale yellowish green upon the addition of leaf extract to the precursor. The continuous heating and stirring to the above solution led to the colour change from pale yellowish green to dark green colour and subsequently the colour changes to blackish brown colour. The above colour change of the solution indicates the formation of CuO NPs. The formed CuO NPs were filtered and dried at 8°C for 30 minutes. The dried yield was stored in an air tight container for further experiments.

Characterization

Ultraviolet – Visible (UV-Vis) spectrum of AuNPs was recorded by Perkin Elmer Lambda 25 Spectrophotometer in 200 – 800 nm range. Fourier Transform Infrared (FT-IR) spectral measurements were performed on JASCO FTIR 410 spectrophotometer in 4000 - 500 cm^{-1} range using KBr pellet technique. SEM (Scanning Electron Microscope) images of the samples were obtained with EVO18 (CARL ZEISS) microscope. EDX (Energy Dispersive X-ray-Spectrometer) elements present in the sample analysed with Quantax 200 with X Flash® 6130.

Antibacterial study

The antibacterial efficacy of the CuO nanoparticles synthesized through green method was evaluated using the Agar-well diffusion technique against a range of pathogenic gram-positive and gram-negative bacteria strains such as *Bacillus cereus*, *Actinomyces israelii*, *Proteus vulgaris*, *Streptococcus pyogenes*, *Corynebacterium diphtheria*, *Pseudomonas aeruginosa*, *Aeromonas hydrophila*, *Propionibacterium acnes*, *Enterococcus faecalis*, and *Staphylococcus aureus*. Indentations (wells ~10mm) were made, and varying concentrations of CuO NPs (500, 250, 100, and 50 $\mu\text{g/ml}$) were introduced into these wells. Subsequently, the plates were incubated at 37°C for

24 hours. The antibacterial effectiveness was assessed by gauging the diameter of the inhibition zone encircling the wells (Bauer *et al.*, 1959). The positive control involved the utilization of the gentamicin antibiotic in this study.

Antifungal study

The synthesized copper oxide nanoparticles were subjected to antifungal assessment by adopting the very same procedure as in antibacterial study. The fungal species used in this study includes *Candida albicans*, *Aspergillus flavus*, *Aspergillus niger* and *Aspergillus fumigatus*. Subsequently, the plates were incubated at 28°C for 72 hours. The assessment of the anti-fungal activity was conducted by measuring the width of the zone of inhibition that formed around the wells (Magaldi *et al.*, 1997; Clinical and Laboratory Standards Institute, 2008). Amphotericin B was employed as a positive control in this experiment.

Antioxidant study

The assessment of in vitro antioxidant activity of CuO nanoparticles synthesized using leaf extract of *Catharanthus roseus* involved DPPH radical scavenging assay. The experiment utilized CuO NPs with standard concentrations of 100, 75, 50, 25, and 10 g/mL . To prevent nanoparticle aggregation, the CuO NPs are sonicated at room temperature for 30 minutes. Absorbance measurement was performed using spectrophotometry, comparing the results with corresponding blank solutions (Manzocco 1998). The percentage of inhibition was calculated using the following formula:

$$\text{Scavenging effect (\% inhibition)} = \left\{ \frac{(\text{Abs of control} - \text{Abs of reaction mix})}{(\text{Abs of control})} \right\} \times 100 \quad (1)$$

In vitro cytotoxicity

The CuO nanoparticles' cytotoxicity assessment utilized the (MTT) assay by Mosmann (1983). HT-29 human colon cancer cells were cultured in Dulbecco's Minimal Essential Medium (DMEM) supplemented with 10% FBS and 1% penicillin-streptomycin solution. Cells (1×10^5 cells per well in 200 μL) were placed in 96-well plates and incubated at 37°C with 5% CO_2 for 24 to 48 hours.

Then, they were treated with various CuO NPs concentrations (10 to 500 µg/mL) for a specific time. MTT solution (10 µL at 5 mg/ml) was added, and after 2-4 hours, distinct purple precipitates were observed and the experiment was carried out in triplicate. After removing the medium and MTT, wells were washed with 1X PBS and formazan crystals obtained was dissolved in 100 µL of DMSO. Absorbance at 570 nm was measured using a microplate reader (Mosmann, 1983; Marshall *et al.*, 1995). The calculation of cell viability percentage was performed using equation (2).

$$\text{Cell viability \%} = \left\{ \frac{\text{mean OD of individual test group}}{\text{mean OD of control group}} \right\} \times 100 \quad (2)$$

Results and discussion

CuO NPs were synthesized by simple green method in which leaf extract of *Catharanthus roseus* is utilized. The phytoconstituents present in the leaf extract serves as both reducing and stabilizing agent for the formation of CuO NPs. The as-prepared metal oxide NPs were characterized by various spectral and analytical tools. A single literature source focused on generating copper oxide nanoparticles at room temperature through *Catharanthus roseus* leaf extract induces as to work on this (Begum *et al.*, 2019). Our study emphasizes on the synthesis of Nps using the leaf extract differently by heating and stirring it with a precursor which led to nanoparticle formation within 5 minutes. This method proves to be uncomplicated and saves time compared to other methods for preparing CuO NPs. The prepared CuO nanoparticles are evaluated for their possible applications in antimicrobial, antioxidant and anticancer investigations.

Spectral features

Absorption studies

The optical absorption characteristic features of CuO nanoparticles were explored at room temperature using UV – visible spectroscopy. The CuO NPs were dissolved in water, underwent analysis via UV–Visible spectroscopy, revealing an absorbance peak at 238 nm, attributed to the Surface Plasmon Resonance (SPR) effect of CuO NPs (Fig. 1). Typically, CuO NPs

exhibit UV-visible absorption within the 200 to 400 nm range, affirming the formation of CuO NPs in this study. In semiconductors, when photons with energy surpassing the semiconductor's gap are absorbed, an electron moves from the valence band to the conduction band (Sathish Kumar *et al.*, 2021, Turakhia *et al.*, 2020).

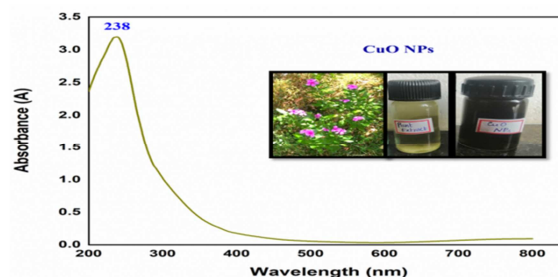


Fig. 1. UV – Vis absorption spectrum of CuO NPs synthesised by using *Catharanthus roseus* leaf extract in aqueous medium

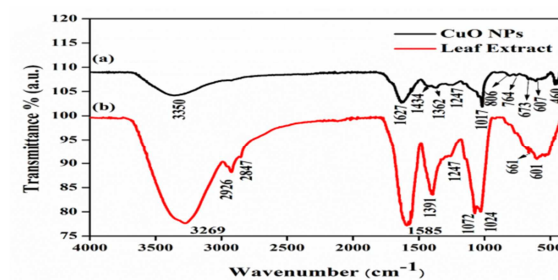


Fig. 2. FT-IR spectra of (a) CuO NPs (b) leaf extract

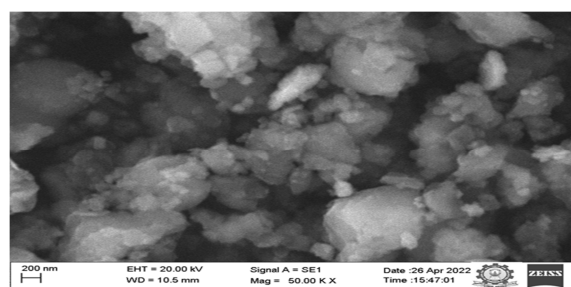


Fig. 3. SEM image of CuO NPs

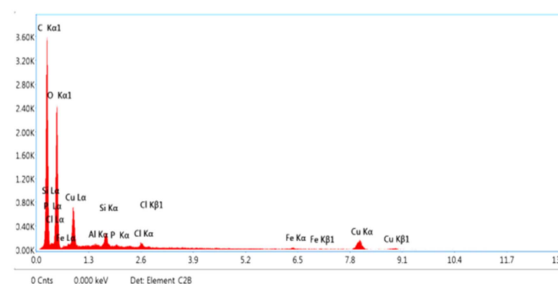


Fig. 4. EDX spectrum of CuO NPs

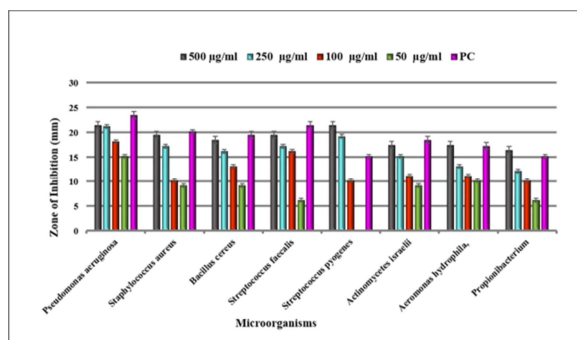


Fig. 5. Zone of inhibition of synthesised CuO NPs against various microorganisms

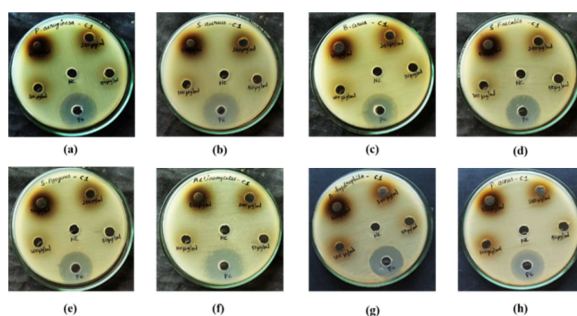


Fig. 6. Antibacterial activity of CuO NPs against gram (+) ve and gram (-)ve strains
 (a) *Pseudomonas aeruginosa* (b) *Staphylococcus aureus* (c) *Bacillus cereus* (d) *Streptococcus faecalis*
 (e) *Streptococcus pyogenes* (f) *Actinomyces israelii* (g) *Aeromonas hydrophila* (h) *Propionibacterium*

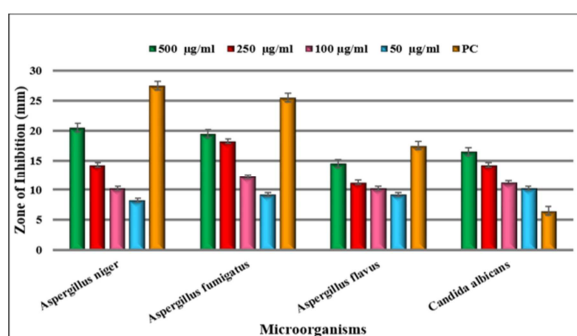


Fig. 7. Zone of inhibition of synthesised CuO NPs against various microorganisms

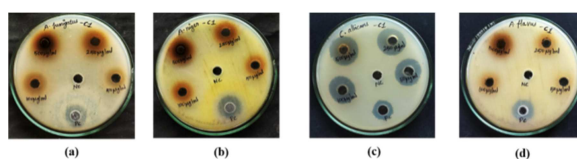


Fig. 8. Microscopic images of Antifungal activity
 (a) *Aspergillus fumigatus* (b) *Aspergillus niger* (c) *Candida albicans* (d) *Aspergillus flavus*

FT-IR characterization

The FT-IR spectrum was recorded in the form of KBr pellet in the region of 4000 – 400 cm⁻¹. Fig. 2a shows the FT-IR spectrum of pure CuO bands appeared at 460, 607, and 673 cm⁻¹ (Subramanian & Subbulekshmi, 2016). The spectra of CuO NPs in the region of 3350 cm⁻¹, the high frequency region indicates -OH stretching in Fig. 2a. The vibrational stretching frequency at 764 cm⁻¹ is assigned for C–H bend of alkenes. The strong band at 1627 cm⁻¹ was assigned to N-H bending of primary and secondary groups of amines and amides. The band at 1434 cm⁻¹ was assigned to –OH bending of carboxylic acid. The red shift was observed from 1017 to 1247 cm⁻¹ which occurred due to oxidation of >C=O groups of the extract components (Begum *et al.*, 2019). A medium band at 1362 cm⁻¹ due to O-H bending of phenol. Similarly, a weak band was observed at 806 cm⁻¹ due to C=C bending of tri substituted alkane. The prominent absorption peak in leaf extract (Fig. 2b) at 3269 cm⁻¹ is linked to the presence of hydroxyl (-OH) functional groups commonly present in alcohols and phenolic compounds. Two medium bands observed at 601 and 661 cm⁻¹ due to C-Cl stretching of halo compounds present in extract. In the region of 1000 to 1300 cm⁻¹, strong bands due to C-O stretching of alcohols, esters, carboxylic acids, anhydrides are present in leaf extract as observed at 1024, 1072 and 1247 cm⁻¹. A strong band at 1391 cm⁻¹ due to S=O stretching of sulfonyl chloride groups and N-H bending vibration spectra observed at 1585 cm⁻¹. In the region 3000-2840 cm⁻¹ two bands present at 2847 and 2926 cm⁻¹ due to C-H stretching of alkanes in Fig. 2b (Amin *et al.*, 2021).

SEM

The SEM image of CuO depicts irregularly shaped particles highly agglomerated together, showcasing nano-spheres, square forms, and clustered structures on the surface. Conversely, the SEM image of CuO NPs in Fig. 3 displays larger, irregularly shaped, spongy-like particles. A closer examination at high magnification (200 nm) reveals the presence of nano clusters covering the entire surface area (Zahrah, 2022).

Table 1. Elemental composition of CuO NPs SEM EDX analysis

Element	Atomic Wt (%)
C	58.3
O	38.6
Al	0.3
Si	0.7
Cl	0.2
P	0.1
Fe	0.2
Cu	1.6

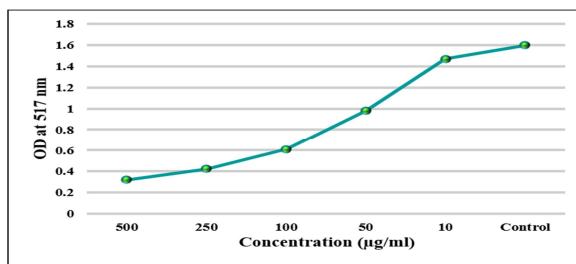


Fig. 9. DPPH radical scavenging activity of CuO NPs of OD value at 517 nm

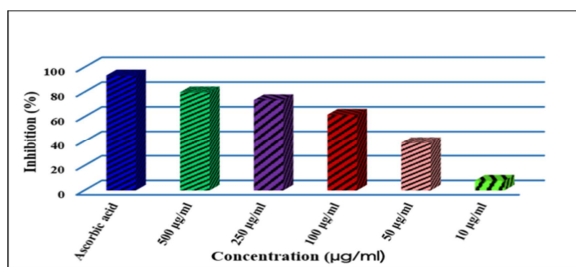


Fig. 10. Inhibition percentage of sample and standard by DPPH

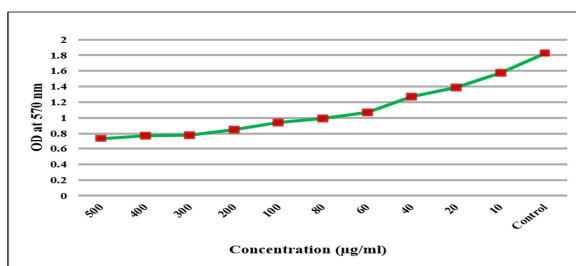


Fig. 11. Absorbance at 570 nm with different concentration of HT-29 Cell lines

EDX

The SEM EDX analysis, (detailed in Table 1) distinctly reveals the elemental composition present in the NPs. The EDX spectrum shown in (Fig. 4) confirms the existence of all components within the CuO NPs. Specifically, the ratio of Cu to O is measured at 1.6% and 38.6%, respectively.

Antibacterial activity of CuO NPs

The antibacterial assessment of copper oxide nanoparticles involved eight different bacterial species, encompassing both gram-positive (+ve) and gram-negative (-ve) types: *Staphylococcus aureus*, *Streptococcus faecalis*, *Streptococcus pyogenes*, *Propionibacterium acnes*, *Pseudomonas aeruginosa*, *Bacillus cereus*, *Aeromonas hydrophila*, and *Actinomyces israelii*. Fig. 5 illustrates the zone of inhibition for CuO NPs against these strains. At 500 µg/ml concentration, the maximum zone of inhibition was observed, measuring 21.5, 19.5, 18.5, 19.5, 21.5, 17.5, 17.5, and 16.5mm, respectively, across the bacterial strains. Notably, *Pseudomonas aeruginosa* displayed higher activity with CuO NPs across all concentrations compared to other bacteria (Al-Jassani & Raheem, 2017; Dadi *et al.*, 2019). Fig. 6 showcases images of the zone of inhibition around the wells for both the antibacterial strains and the synthesized CuO NPs. The results were tabulated and compared with a standard, Gentamicin positive control as depicted in Table 2.

Antifungal activity of CuO NPs

The biosynthesized CuO NPs underwent antifungal assessment using the agar well diffusion method against various pathogens, including two gram-positive fungal species *Candida albicans* and *Aspergillus flavus* and two gram-negative fungal species *Aspergillus niger* and *Aspergillus fumigatus*. The results indicated that the maximum zone of inhibition across all strains at 500 µg/mL of CuO NPs, measuring 20.52, 19.5, 14.5, and 16.5 mm, respectively. Notably, *Aspergillus fumigatus* displayed high inhibition zones across concentrations of 500, 250, 100, and 50 µg/mL, as shown in Fig. 7. The disk diffusion method validated the antifungal activity of CuO NPs, illustrated by images of the inhibition zones around the wells in Fig. 8. The activity against *Candida albicans* surpassed that of the reference standard, Amphotericin B positive control. The detailed results about the zone of inhibition were tabulated in Table 3.

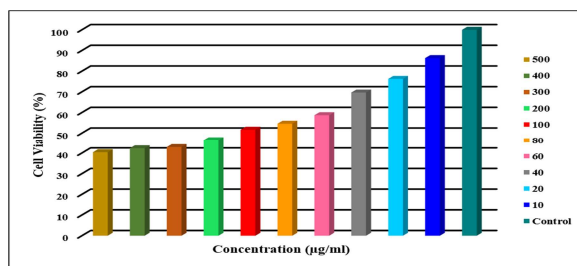


Fig. 12. Cell viability % of HT-29 cell lines

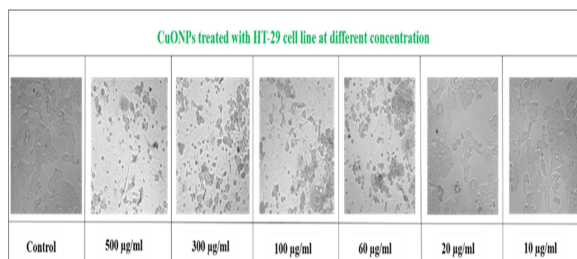


Fig. 13. Cytotoxicity study of CuO NPs of HT-29 cell line

Antioxidant activity of Copper nanoparticles

The radical scavenging capability of the synthesized copper oxide nanoparticles was assessed through the in vitro DPPH assay. Table 4 and Fig. 9 depict the optical density of the synthesized CuO NPs alongside the control (Ascorbic acid) values. These results were then tabulated in Table 5, where the free radical scavenging activity at various nanoparticle concentrations was compared, revealing an IC₅₀ value of 58.55 µg/mL. The results in Table 4 and 5

highlighted the potent inhibition of DPPH by CuO nanoparticles. Furthermore, Fig. 10 illustrates the dose-dependent percentage inhibition response of CuO-NPs and ascorbic acid against the DPPH radical.

In vitro cytotoxicity

The in vitro assessment of the synthesized copper oxide nanoparticles targeted the HT-29 human colon cancer cell line through the MTT assay for anticancer activity. Triplicate tests with different concentrations (10, 20, 40, 60, 80, 100, 200, 300, 400, and 500 µg/mL) of CuO nanoparticles were conducted over 48 hours. The obtained optical density values at 570 nm against the control were tabulated in Table 6 and plotted in Fig. 11. Cell viability was concentration-dependent, declining as the sample concentration increased (Table 7). The concentration-dependent curves of CuO nanoparticles revealed significant cytotoxicity, exhibiting an IC₅₀ value of 37.99 µg/mL against the tested cancer cell line. Notably, lower concentrations of CuO NPs showed higher cell viability percentages and optical density values. Fig. 12 demonstrates the considerable cytotoxicity of cell viability percentages at concentrations of 10, 20 and 40 µg/mL of synthesized CuO NPs—measuring 86%, 76%, and 69%, respectively. Moreover, Fig. 13 illustrates the microscopic images exhibiting the anticancer activity of CuO NPs against the HT-29 human colon cancer cell line.

Table 2. Different concentration of sample zone of inhibition

SL	Name of the organism	Zone of inhibition (mm), Mean±SD				
		500 µg/ml	250 µg/ml	100 µg/ml	50 µg/ml	PC
1.	<i>Pseudomonas aeruginosa</i>	21.5±0.707	21.25±0.35	18.25±0.30	15.25±0.3	23.5±0.707
2.	<i>Staphylococcus aureus</i>	19.5±0.70	17.25±0.35	10.25±0.30	7.25±0.3	20.25±0.35
3.	<i>Bacillus cereus</i>	18.5±0.707	16.25±0.35	13.25±0.3	9.25±0.3	19.5±0.707
4.	<i>Streptococcus faecalis</i>	19.5±0.707	17.25±0.35	16.25±0.35	6.25±0.3	21.5±0.7
5.	<i>Streptococcus pyogenes</i>	21.5±0.707	19.25±0.35	10.25±0.3	0	15.25±0.35
6.	<i>Actinomyces israelii</i>	17.5±0.7071	15.25±0.35	11.25±0.3	9.25±0.3	18.5±0.7071
7.	<i>Aeromonas hydrophila</i> ,	17.5±0.707	13.25±0.3	11.25±0.3	10.25±0.30	17.5±0.707
8.	<i>Propionibacterium acnes</i>	16.5±0.70	12.25±0.35	10.25±0.30	6.25±0.30	15.25±0.35

*PC is Gentamicin

Table 3. Antifungal activity of CuO NPs

SL	Name of the test organism	Zone of inhibition (mm), SD ± Mean				
		500 µg/ml	250 µg/ml	100 µg/ml	50 µg/ml	PC
1.	<i>Aspergillus niger</i>	20.5±0.70	14.25±0.35	10.25±0.30	8.25±0.3	27.5±0.707
2.	<i>Aspergillus fumigatus</i>	19.5±0.707	18.25±0.35	12.25±0.3	9.25±0.3	25.5±0.70
3.	<i>Aspergillus flavus</i>	14.5±0.70	11.25±0.35	10.25±0.3	9.25±0.3	17.5±0.707
4.	<i>Candida albicans</i>	16.5±0.707	14.25±0.35	11.25±0.30	10.25±0.3	6.5±0.70

*PC is Amphotericin B

Table 4. Different concentration of sample OD Value at 517 nm

SL	Sample concentration (µg/ml)	OD Value at 517 nm (in triplicate)			Mean
1	500	0.314	0.314	0.314	0.319
2	250	0.422	0.422	0.422	0.421
3	100	0.472	0.472	0.472	0.609
4	50	0.802	0.802	0.802	0.978
5	10	1.440	1.440	1.440	1.469
6	Control	1.564	1.564	1.564	1.595

Table 5. Percentage of inhibition of CuO NPs

SL	Sample concentration (µg/ml)	Percentage of inhibition (in triplicate)			Mean
1.	Ascorbic acid	94.98433	94.98433	94.98433	93.52142
2.	500	80.31348	80.31348	80.31348	79.9582
3.	250	73.54232	73.54232	73.54232	73.60502
4.	100	70.40752	70.40752	70.40752	61.83908
5.	50	49.71787	49.71787	49.71787	38.70428
6.	10	9.717868	9.717868	9.717868	7.920585

Table 6. Absorbance Value at 570 nm with different concentrations

SL	Tested sample concentration (µg/ml)	OD value at 570 nm (in triplicate)			Mean
1	500	0.708	0.708	0.708	0.737
2	400	0.77	0.77	0.77	0.771
3	300	0.781	0.781	0.781	0.782
4	200	0.813	0.813	0.813	0.849
5	100	0.927	0.927	0.927	0.942
6	80	0.99	0.99	0.99	0.995
7	60	1.06	1.06	1.06	1.07
8	40	1.212	1.212	1.212	1.271
9	20	1.373	1.373	1.373	1.390
10	10	1.521	1.521	1.521	1.574
11	Control	1.737	1.737	1.737	1.824

Table 7. Cell Viability (%) of HT-29 cell line

SL	Tested sample concentration (µg/ml)	Cell viability (%) (in triplicate)			Mean (%)
1	500	40.7599	40.7599	40.7599	40.402231
2	400	44.3293	44.3293	44.3293	42.36001
3	300	44.9626	44.9626	44.9626	42.945746
4	200	46.8048	46.8048	46.8048	46.520236
5	100	53.3679	53.3679	53.3679	51.684592
6	80	56.9948	56.9948	56.9948	54.61429
7	60	61.0248	61.0248	61.0248	58.726324
8	40	69.7755	69.7755	69.7755	69.683741
9	20	79.0443	79.0443	79.0443	76.265166
10	10	87.5648	87.5648	87.5648	86.323426
11	Control	100	100	100	100

Conclusion

The study presents a cost-effective and efficient synthesis of copper oxide nanoparticles using *Catharanthus roseus* leaf extract. Various analyses including UV-Vis spectroscopy, FTIR, SEM and EDX validated the reduction of copper chloride to copper oxide nanoparticles and revealed specific characteristics. CuO NPs exhibited potent antibacterial activity against *Pseudomonas aeruginosa* and impressive antifungal effect against *Candida albicans*, surpassing Amphotericin B.

They also displayed robust DPPH inhibition (IC₅₀: 58.55 µg/mL), showcasing significant antioxidant potential. The HT-29 cancer cell line showed reduced viability with increasing CuO nanoparticle concentrations, indicating the toxicity (IC₅₀: 37.99 µg/mL).

This study demonstrates the vast potential of these CuO nanoparticles as an ideal candidate for antibacterial, antifungal, antioxidant and anticancer applications.

Acknowledgement

The authors gratefully acknowledge the instrumental facility provided by the Department of Chemistry supported by DST-FIST Level I Phase II Project (SR/FST/CSI-247/2012).

References

Al-Jassani MJ, Raheem HQ. 2017. Anti-bacterial activity of CuO nanoparticles against some pathogenic bacteria. *Int. J. Chem. Tech. Res* **10(2)**, 818-822.

Alahdal FA, Qashqoosh MT, Manea YK, Mohammed RK, Naqvi S. 2023. Green synthesis and characterization of copper nanoparticles using *Phragmanthera austroarabica* extract and their biological/environmental applications. *Sustainable Materials and Technologies* **35**, e00540.

Amin F, Khattak B, Alotaibi A, Qasim M, Ahmad I, Ullah R, Ahmad R. 2021. Green synthesis of copper oxide nanoparticles using *Aerva javanica* leaf extract and their characterization and investigation of in vitro antimicrobial potential and cytotoxic activities. *Evidence-Based Complementary and Alternative Medicine* 2021, 5589703. <https://doi.org/10.1155/2021/5589703>

Bhavyasree PG, Xavier TS. 2022. Green synthesised copper and copper oxide based nanomaterials using plant extracts and their application in antimicrobial activity. *Current Research in Green and Sustainable Chemistry* **5**, 100249.

Bajwa N, Mahal S, Singh PA, Jyoti K, Dewangan P, Madan J, Baldi A. 2023. Drug-polymer conjugates: Challenges, opportunities, and future prospects in clinical trials. *Polymer-Drug Conjugates*, 389-469p.

Bauer AW, Roberts Jr CE, Kirby WM. 1959. Single disc versus multiple disc and plate dilution techniques for antibiotic sensitivity testing. *Antibiotics Annual* **7**, 574-580.

Begum SN, Esakkiraja A, Asan SM, Muthumari M, Raj GV. 2019. Green Synthesis of Copper Oxide Nanoparticles Using *Catharanthus roseus* Leaf Extract and Their Antibacterial Activity. *Int. J. Sci. Res. in Multidisciplinary Studies* **5**, 8.

Chakraborty N, Banerjee J, Chakraborty P, Banerjee A, Chanda S, Ray K, Sarkar J. 2022. Green synthesis of copper/copper oxide nanoparticles and their applications: a review. *Green Chemistry Letters and Reviews* **15(1)**, 187-215.

Clinical and Laboratory Standards Institute. 2008. Reference method for broth dilution antifungal susceptibility testing of yeasts. Approved Standard M27-A3.

Dadi R, Azouani R, Traore M, Mielcarek C, Kanaev A. 2019. Antibacterial activity of ZnO and CuO nanoparticles against gram positive and gram-negative strains. *Materials Science and Engineering: C* **104**, 109968.

Darroudi M, Ahmad MB, Abdullah AH, Ibrahim NA. 2011. Green synthesis and characterization of gelatin-based and sugar-reduced silver nanoparticles. *International Journal of Nanomedicine*, 569-574p.

Gahlawat G, Choudhury AR. 2019. A review on the biosynthesis of metal and metal salt nanoparticles by microbes. *RSC advances* **9(23)**, 12944-12967.

Rajbhoj A. 2011. Copper Oxide Nanoparticles: Synthesis, Characterization, and Their Antibacterial Activity, *Journal of Cluster Science*, 22, 121-129.

Jabarkhil M, Azizi AS, Imam SZ, Alrabbat A, Hasan KD, Hasan MH. 2023. Revolutionising Cancer Diagnosis and Treatment: A Review on Advancements in Nanomaterial-based Theranostics. *International Journal of Engineering Materials and Manufacture* **8(4)**, 106-123.

- Manimaran K, Yuli Yanto DH, Kamaraj C, Selvaraj K, Pandiaraj S, Elgorban AM, Vignesh S, Kim H.** 2023. Eco-friendly approaches of mycosynthesized copper oxide nanoparticles (CuONPs) using *Pleurotus citrinopileatus* mushroom extracts and their biological applications. *Environmental Research* **232**, 116319.
- Magaldi D, Silvia W, Camero T.** 1997. Suceptibilidad de *Candida albicans* "In vitro" mediante los posos de diffusion. *Bol. venez. Infectol* 5-8p.
- Manzocco L, Anese M, Nicoli MC.** 1998. Antioxidant properties of tea extracts as affected by processing. *LWT-Food Science and Technology* **31**, 694-698.
- Mosmann T.** 1983. Rapid colorimetric assay for cellular growth and survival: application to proliferation and cytotoxicity assays. *Journal of Immunological Methods* **65**, 55-63.
- Marshall NJ, Goodwin CJ, Holt SJ.** 1995. A critical assessment of the use of microculture tetrazolium assays to measure cell growth and function. *Growth regulation* **5**, 69-84.
- Rajagopal G, Nivetha A, Sundar M, Panneerselvam T, Murugesan S, Parasuraman P, Kunjiappan S.** 2021. Mixed phytochemicals mediated synthesis of copper nanoparticles for anticancer and larvicidal applications. *Heliyon* **7(6)**.
- Siddiquee MA, Parray MD, Kamli MR, Malik MA, Mehdi SH, Imtiyaz K, Rizvi MM, Rajor HK, Patel R.** 2021. Biogenic synthesis, in-vitro cytotoxicity, esterase activity and interaction studies of copper oxide nanoparticles with lysozyme. *Journal of Materials Research and Technology* **13**, 2066-2077.
- Saleh HM, Hassan AI.** 2023. Synthesis and characterization of nanomaterials for application in cost-effective electrochemical devices. *Sustainability* **15(14)**, 10891.
- Sajid M, Plotka-Wasyłka J.** 2020. Nanoparticles: Synthesis, characteristics, and applications in analytical and other sciences. *Microchemical Journal* **154**, 104623.
- Sardar R, Ahmed S, Shah AA, Yasin NA.** 2022. Selenium nanoparticles reduced cadmium uptake, regulated nutritional homeostasis and antioxidative system in *Coriandrum sativum* grown in cadmium toxic conditions. *Chemosphere* **287**, 132332.
- Subramanian E, Subbulekshmi NL.** 2016. Copper Oxide Incorporated Zeolite Catalyst Developed from Waste Coal Fly Ash Material and Its Catalytic Wet Peroxide Oxidative Degradation of Crystal Violet Dye. *Journal of Advanced Chemical Sciences* **1**, p. 204-207.
- Sathish Kumar K, Raghavendra R, Mohamed Khalith SB, Mohammed Junaid Hussain D, Darul Raiyaan GI, Kantha Deivi A.** 2021. Characterization, antibacterial and photocatalytic evaluation of green synthesized copper oxide nanoparticles. *Biocatalysis and Agricultural Biotechnology* **31**, 101904.
- Turakhia B, Divakara MB, Santosh MS, Shah S.** 2020. Green synthesis of copper oxide nanoparticles: A promising approach in the development of antibacterial textiles. *Journal of Coatings Technology and Research* **17**, 531-540.
- Thambidurai S, Gowthaman P, Venkatachalam M, Suresh S.** 2020. Enhanced bactericidal performance of nickel oxide-zinc oxide nanocomposites synthesized by facile chemical co-precipitation method. *Journal of Alloys and Compounds* **830**, 154642.
- Zahrah A.** 2022. Green synthesis of copper oxide nanoparticles CuO NPs from *Eucalyptus globoulus* leaf extract: Adsorption and design of experiments. *Arabian Journal of Chemistry* **15**, 103739.